

Cite this: *RSC Adv.*, 2019, 9, 8529

# A highly selective colorimetric fluorescent probe for detection of $\text{Hg}^{2+}$ and its application on test strips

Geng Yang,<sup>a</sup> Xia Meng,<sup>a</sup> Shimin Fang,<sup>a</sup> Hongdong Duan,<sup>ID</sup>\*<sup>a</sup> Lizhen Wang<sup>ID</sup>\*<sup>b</sup> and Zhenzheng Wang<sup>a</sup>

An efficient fluorescent probe **Pyr-Rhy** based on pyrazole was developed, which can detect  $\text{Hg}^{2+}$  in water. Its fluorescence properties were studied by UV-vis and fluorescence spectroscopy, and the study results indicated that this probe can selectively detect  $\text{Hg}^{2+}$  via complexation reaction, and then cause a remarkable color change from colorless to pink and a strong fluorescence enhancement can be observed. Furthermore, this probe showed high sensitivity with the detection limit down to  $2.07 \times 10^{-8}$  M, and its stoichiometric ratio toward  $\text{Hg}^{2+}$  ions was 1 : 1. The sensing mechanism was investigated by Job's plot  $^1\text{H}$  NMR titrations, and FT-IR spectra analysis, which demonstrated a chelation-enhanced fluorescence (CHEF) mechanism. More importantly, obvious color changes of sensor **Pyr-Rhy** can be observed when it was impregnated on filter paper testing strips and immersed in  $\text{Hg}^{2+}$  solution (water as solution), indicating its potential application for trace  $\text{Hg}^{2+}$  detection in environmental samples.

Received 30th January 2019

Accepted 2nd March 2019

DOI: 10.1039/c9ra00797k

rsc.li/rsc-advances

## 1. Introduction

Mercury (Hg), one of the most toxic pollutants,<sup>1</sup> is widely distributed in the environment and exists in the state of mercury metal, inorganic mercury and organic mercury compounds.<sup>2,3</sup> The organic mercury is the most harmful of the mercury-containing compounds, because it is hardly biodegradable and can be biomagnified in the food chain.<sup>4</sup> Even at very low levels, organic mercury can seriously destroy the activity of proteins and enzymes, thereby causing various diseases, including brain damage, movement disorders, cognitive dysfunction and kidney failure.<sup>5–7</sup> There are many previous studies for the detection of mercury ions with different methods, and we have compared the present method with the others, and a table was added (Table 1).<sup>8–11</sup> While other methods can detect  $\text{Hg}^{2+}$ , they can't be reused; and the synthesis methods of other methods are cumbersome and not easy to operate. Therefore, it is necessary to develop a sensitive, fast and low-cost method for detection of  $\text{Hg}^{2+}$ .

In recent years, there have been many ways to detect cations and anions such as ratiometric fluorescent paper sensor,<sup>12</sup> silica-based SERS chip.<sup>13,14</sup> Schiff base fluorescent probes have

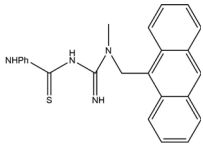
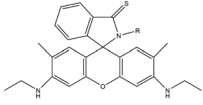
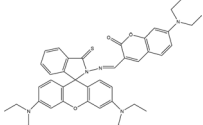
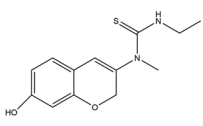
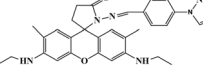
been drawn great attention and widely used in detection of heavy metal ions.<sup>15</sup> The C=N structure in Schiff base has strong chelating ability, and more importantly, these chelating processes always produce strong fluorescence release.<sup>16,17</sup> Pyrazole derivatives are interesting heterocyclic compounds bearing five membered heterocycles and useful raw materials to synthesize various biological molecules. Due to their strong coordination ability with metal ions, pyrazole based derivatives have been widely used for the development of fluorescent probes to detect heavy metal ions, such as  $\text{Zn}^{2+}$ ,  $\text{Cd}^{2+}$ , and  $\text{Hg}^{2+}$ .<sup>18–20</sup> Furthermore, pyrazole derivatives are always employed as important capping motifs in probing molecules, which can be used as ligands for selective recognition metal ions in coordination chemistry. Therefore, pyrazoles are attracting building blocks for designing and synthesizing a series of heterocyclic compounds, such as optical brighteners, and UV stabilizers, and fluorescent probes.<sup>21</sup>

In this paper, a novel fluorescent probe **Pyr-Rhy** was described, which was synthesized by modification of rhodamine with a pyrazole derivative (Fig. 1). This probe exhibited high fluorescent “turn-on” response toward  $\text{Hg}^{2+}$  in aqueous DMSO solution, and this process was accompanied with a sensitive fluorescence color change that could not be interfered by other coexisting metal ions. Test results showed that the recognition process of sensor **Pyr-Rhy** toward  $\text{Hg}^{2+}$  was completed instantly, and the detection limit was found to be as low as  $2.07 \times 10^{-8}$  M. Therefore, sensor **Pyr-Rhy** could be used for quantitative estimation of  $\text{Hg}^{2+}$  in aqueous media.

<sup>a</sup>School of Chemistry and Pharmaceutical Engineering, Qilu University of Technology (Shandong Academy of Sciences), Ji'nan, Shandong Province, China 250300. E-mail: hdduan67@163.com; Tel: +86 13153035598

<sup>b</sup>Biology Institute, Qilu University of Technology (Shandong Academy of Sciences), Ji'nan, Shandong Province, China 250014. E-mail: wlzh1106@126.com; Tel: +86 15866683436

Table 1 Compared the present method with the others

| Structural of compound  | Molecular formula   | Solvent   | Repeatability | Reference |
|---|---|---|---------------|-----------|
|  | C <sub>24</sub> H <sub>22</sub> N <sub>4</sub> S                | Acetonitrile  | No            | 8         |
|  | C <sub>27</sub> H <sub>29</sub> N <sub>3</sub> OSR              | PBS buffer (containing 20% DMF as a co-solvent)       | No            | 9         |
|  | C <sub>42</sub> H <sub>45</sub> N <sub>5</sub> O <sub>3</sub> S | Ethanol/water, (1 : 1)                                | No            | 10        |
|  | C <sub>13</sub> H <sub>12</sub> N <sub>2</sub> O <sub>2</sub> S | 0.5 M H <sub>2</sub> SO <sub>4</sub> aqueous solution | No            | 11        |
|  | C <sub>3</sub> H <sub>34</sub> N <sub>6</sub> O <sub>2</sub>    | DMSO/H <sub>2</sub> O (1/1, v/v)                      | Yes           | This work |

## 2. Materials and methods

### 2.1. General information

In this experiment unless otherwise noted, all reagents and materials were derived from commercial, which without further refinement. Pyrazole, *p*-fluorobenzaldehyde, rhodamine 6G, hydrazine hydrate and glacial acetic acid were purchased from Aladdin. Distilled water was produced in our lab. Different metal ion solutions were prepared with the corresponding inorganic salts. Nuclear magnetic spectrometer is Bruker AV-400 spectrometer; infrared spectrometer is Bruker ALPHA FT-IR spectrometer fluorospectrophotometer is Hitachi F-4600 and scanning speed was 2400 nm min<sup>-1</sup>.

### 2.2. Synthesis

**2.2.1 Synthesis of compound 1.** Pyrazole (1.36 g, 20 mmol), *p*-fluorobenzaldehyde (2.48 g, 20 mmol) and anhydrous

potassium carbonate (6.90 g, 50 mmol) were dissolved in 50 mL of DMF, the mixture was allowed to warm 110 °C and stirred at this ambient temperature for 24 h. After TLC showed the conversion of the starting material, the mixture was cooled to room temperature, filtered.<sup>22</sup> The filtrate was diluted with 400 mL of distilled water and the mixture was extracted with 100 mL of acetic ether, the organic layer was dried with anhydrous sodium sulfate and then evaporated, the resultant residue was purified by a column chromatography (petroleum/ethyl acetate, 7/1) to give compound 1 was a white powder (3.34 g, yield 91%); mp 82–84 °C; <sup>1</sup>H NMR (400 MHz, DMSO-*d*<sub>6</sub>) δ 10.00 (s, 1H), 8.68 (d, *J* = 2.5 Hz, 1H), 8.06 (dd, *J* = 8.7 Hz, 4H), 7.85 (t, *J* = 6.4 Hz, 1H), 6.67–6.58 (m, 1H); <sup>13</sup>C NMR: (100 MHz, DMSO-*d*<sub>6</sub>) δ 191.87, 143.67, 142.21, 133.65, 131.15, 128.44, 118.27, 108.88 ppm; ESI-TOF HRMS (*m/z*): calcd for C<sub>10</sub>H<sub>8</sub>N<sub>2</sub>O<sup>+</sup>, [M + H]<sup>+</sup>, 172.0729; found, 172.0731.

**2.2.2 Synthesis of compound 3.** To the mixture of rhodamine 6G 2 (9.85 g, 20 mmol) in 300 mL of ethanol was added an

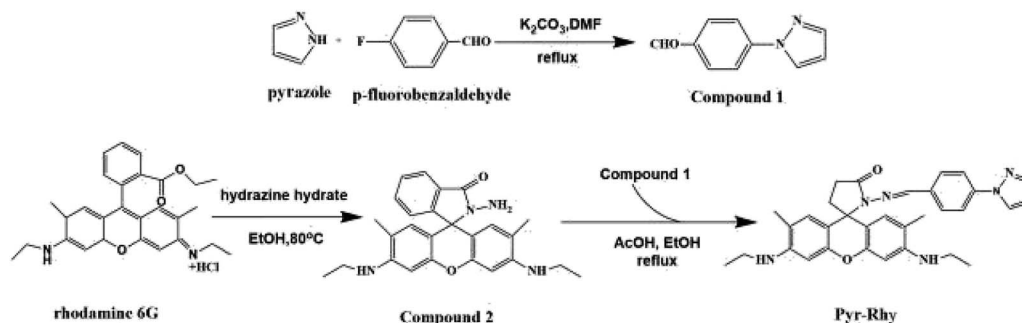


Fig. 1 Synthesis of pyrazole-based fluorescent probe Pyr-Rhy.



excess of hydrazine hydrate (0.95 g, 20 mmol), the mixture was heated to 80 °C and refluxed for 12 h to give a dark red clear transparent solution. Then, the mixture was subjected to decompression and evaporation till a few solid was formed. After which, the mixture was poured into 200 mL of deionized water, rested for 3 hours, and filtered.<sup>23</sup> The solid was washed alternately with distilled water and ethanol several times, and dried *in vacuo* to afford compound 3 as a pink solid (7.88 g, yield 70%); <sup>1</sup>H NMR (400 MHz, DMSO-*d*<sub>6</sub>) δ 7.79–7.71 (m, 1H), 7.50–7.41 (m, 2H), 6.98–6.87 (m, 1H), 6.26 (s, 2H), 6.10 (s, 2H), 4.99 (t, *J* = 5.3 Hz, 2H), 4.21 (s, 2H), 3.32 (s, 1H), 1.88 (d, *J* = 9.9 Hz, 6H), 1.21 (t, *J* = 7.0 Hz, 6H); <sup>13</sup>C NMR: (100 MHz, DMSO-*d*<sub>6</sub>) δ 165.19, 152.05, 151.33, 147.34, 132.27, 129.47, 127.98, 126.98, 123.40, 122.11, 117.77, 105.00, 95.86, 64.95, 37.44, 17.01, 14.19 ppm; ESI-TOF HRMS (*m/z*): calcd for C<sub>26</sub>H<sub>28</sub>N<sub>4</sub>O<sub>2</sub>, [M + H]<sup>+</sup>, 429.22; found, 429.64.

**2.2.3 Synthesis of sensor Pyr-Rhy.** Compound 3 (1.72 g, 10 mmol) and compound 1 (4.56 g, 10 mmol) were dissolved in 40 mL of ethanol, the mixture was heated to 80 °C and refluxed for 2 h after a catalytic amount of acetic acid (3.46 mL, 10 mmol) was added. Then the mixture was cooled to room temperature to yield a rose pink precipitate. The mixture was filtered, the solid was washed with ethanol for several times and dried *in vacuo* to give sensor **Pyr-Rhy** (4.98 g, yield 79.3%); <sup>1</sup>H NMR (400 MHz, DMSO-*d*<sub>6</sub>) δ 8.60 (s, 1H), 8.36 (d, *J* = 2.4 Hz, 1H), 7.78 (d, *J* = 7.0 Hz, 1H), 7.70 (d, *J* = 8.6 Hz, 2H), 7.61 (d, *J* = 1.3 Hz, 1H), 7.52–7.33 (m, 4H), 6.92 (d, *J* = 7.3 Hz, 1H), 6.44–6.37 (m, 1H), 6.21 (s, 2H), 6.05 (s, 2H), 4.94 (t, *J* = 5.3 Hz, 2H), 4.22 (t, *J* = 5.1 Hz, 1H), 1.07 (t, *J* = 7.1 Hz, 6H), 0.92 (t, *J* = 7.0 Hz, 4H); <sup>13</sup>C NMR: (100 MHz, DMSO-*d*<sub>6</sub>) δ 164.36–164.05, 152.00–151.71, 151.48, 148.30, 146.45–146.22, 142.08–141.78, 141.17–140.81, 134.52–134.16, 132.50, 129.50–129.00, 128.29, 127.35, 124.49–124.07, 123.62–122.94, 118.82, 108.75, 105.45, 96.22, 66.05, 37.95, 19.18–18.89, 17.48, 14.64 ppm; ESI-TOF HRMS (*m/z*): calcd for C<sub>32</sub>H<sub>34</sub>N<sub>6</sub>O<sub>2</sub>, [M + H]<sup>+</sup>, 534.66; found, 534.68.

### 3. Results and discussion

#### 3.1. UV-vis absorption spectral studies of sensor Pyr-Rhy

The UV-vis absorption spectra of sensor **Pyr-Rhy** toward different metal ions (Ag<sup>+</sup>, Al<sup>3+</sup>, Cd<sup>2+</sup>, Co<sup>2+</sup>, Cr<sup>3+</sup>, Cu<sup>2+</sup>, Hg<sup>2+</sup>, Mg<sup>2+</sup>, Ni<sup>2+</sup> and Zn<sup>2+</sup>) were studied through using UV-vis spectroscopy.<sup>24,25</sup> As shown in Fig. 2, free sensor solution in DMSO/H<sub>2</sub>O (1/1, v/v) showed one distinct absorption band at 320 nm. However, with the addition of Hg<sup>2+</sup> (10 μM, water as solution) to the above solution, a new the observed absorption band at 320 nm decreased obviously. Whereas, with the addition of other metal cations (Ag<sup>+</sup>, Al<sup>3+</sup>, Cd<sup>2+</sup>, Co<sup>2+</sup>, Cr<sup>3+</sup>, Cu<sup>2+</sup>, Mg<sup>2+</sup>, Ni<sup>2+</sup> and Zn<sup>2+</sup>, water as solution) showed no significant decrease, which indicated the complexation of sensor **Pyr-Rhy** with Hg<sup>2+</sup>. These test results displayed that the UV-vis response of sensor **Pyr-Rhy** has highly specific selection for Hg<sup>2+</sup>.

#### 3.2. Fluorescence study of sensor Pyr-Rhy

The fluorescence emission behavior of sensor **Pyr-Rhy** toward different metal ions was investigated in DMSO/H<sub>2</sub>O (1/1, v/v)

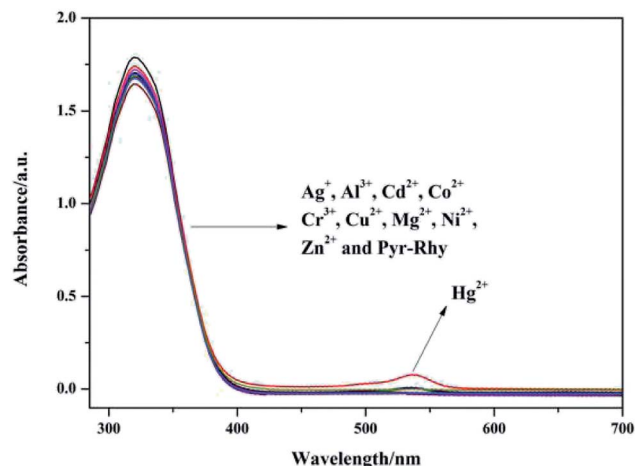


Fig. 2 UV-vis absorption spectra of sensor **Pyr-Rhy** (10 μM) upon addition of different metal ions (10 μM) in DMSO/H<sub>2</sub>O (1/1, v/v) solution.

solution, and the test results can be seen from Fig. 3.<sup>26–28</sup> Clearly, free sensor **Pyr-Rhy** exhibited one fluorescence emission band at about 575 nm with an excitation at 525 nm. But after the addition of Hg<sup>2+</sup> (1.0 equiv.), a significant fluorescence enhancement can be observed with the emission maximum at 575 nm. In contrast, addition of other metal ions exhibited no significant fluorescence enhancement. This fluorescence response of sensor **Pyr-Rhy** to Hg<sup>2+</sup> might be ascribed to the blocked photoinduced electron transfer (PET) process and the chelation-enhanced fluorescence (CHEF) behavior.<sup>29,30</sup> Before adding metal ions, the isomerization of C=N double bond of sensor **Pyr-Rhy** exhibited weak fluorescence emission. While, addition of metal ions led to a new π-conjugated structure, which was accompanied with a selective chelation-enhanced fluorescence (CHEF) effect.

The specificity of sensor **Pyr-Rhy** toward Hg<sup>2+</sup> was investigated by colorimetric experiments. As we can see from Fig. 4a, addition of Hg<sup>2+</sup> to the solution of sensor **Pyr-Rhy** in DMSO/H<sub>2</sub>O

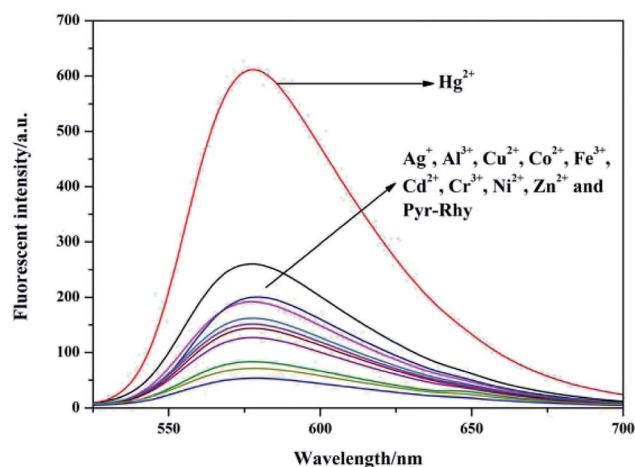


Fig. 3 Fluorescence spectra of sensor **Pyr-Rhy** (10 μM) in the presence of various metal ions (10 μM) in DMSO/H<sub>2</sub>O (1/1, v/v) solution ( $\lambda_{\text{ex}}$  = 525 nm).





Fig. 4 (a) Colorimetric performance of sensor Pyr-Rhy (10  $\mu\text{M}$ ) upon addition of different metal ions (1.0 equiv.) in DMSO/ $\text{H}_2\text{O}$  (1/1, v/v) solution; (b) color change induced upon addition of  $\text{Hg}^{2+}$  under 365 nm UV lamp.



Fig. 5 (a) The fluorescence spectra of sensor Pyr-Rhy (10  $\mu\text{M}$ ) with the increasing concentration of  $\text{Hg}^{2+}$  ion (0–2.0 equiv.) in ethanol solution; (b) the linear fit between sensor Pyr-Rhy and  $\text{Hg}^{2+}$  ion.

(10  $\mu\text{mol L}^{-1}$ , 1/99, v/v) resulted in a color change from colorless to pink in a few seconds, which suggested that sensor Pyr-Rhy could be used for naked eye recognition of  $\text{Hg}^{2+}$  with concentration as low as 10  $\mu\text{mol L}^{-1}$ . In addition, the fluorescence color change from blond to bright yellow was clearly observed

under 365 nm UV light after addition of  $\text{Hg}^{2+}$ . Addition of other metal cations showed no distinct influence on the fluorescence color (Fig. 4b). These outstanding findings demonstrated that

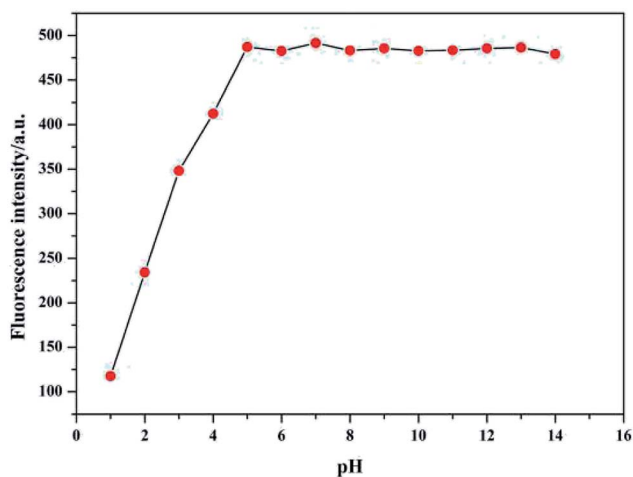


Fig. 6 Effect of pH on the fluorescence intensity of sensor Pyr-Rhy toward  $\text{Hg}^{2+}$  in DMSO/ $\text{H}_2\text{O}$  (1/1, v/v) solution.

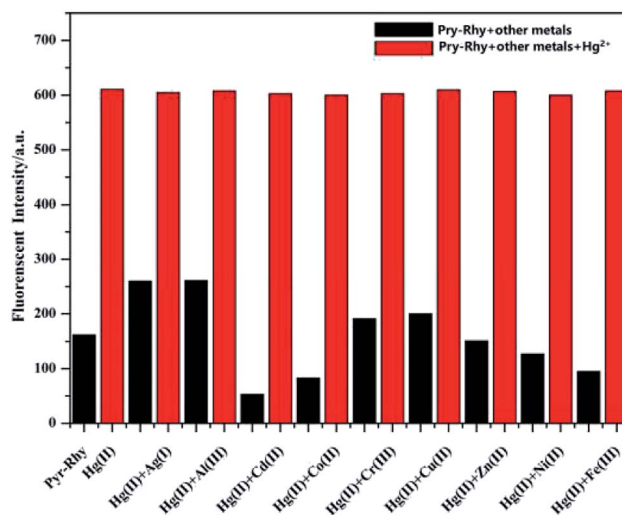


Fig. 7 The black bars represent the fluorescent intensity of sensor Pyr-Rhy and various metal ions (1.0 equiv.) in DMSO/ $\text{H}_2\text{O}$  (1/1, v/v) solution; the red bars represent the fluorescent intensity of sensor Pyr-Rhy and  $\text{Hg}^{2+}$  (1.0 equiv.) in DMSO/ $\text{H}_2\text{O}$  (1/1, v/v) solution.





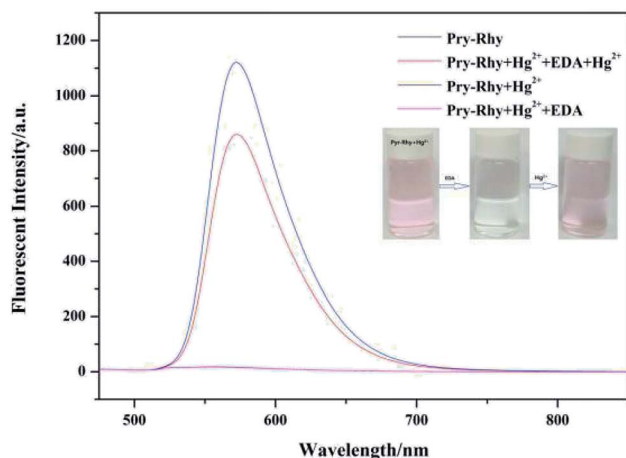


Fig. 8 Changes in emission spectra of **Pyr-Rhy** in the presence of  $\text{Hg}^{2+}$  and EDA in ethanol solution. Inset: color change induced upon addition of EDA.

sensor **Pyr-Rhy** could be used to detect  $\text{Hg}^{2+}$  qualitatively and quantitatively by changing the color and doubling the spectral signals.

To explore the sensitivity of sensor **Pyr-Rhy** toward  $\text{Hg}^{2+}$ , the fluorescence titration experiments were carried out and the results were shown in Fig. 5a. The fluorescence intensity of sensor **Pyr-Rhy** was gradually enhanced with the increasing of  $\text{Hg}^{2+}$  concentration. It was clearly found that the saturation state was reached in presence of 1.0 equiv. of  $\text{Hg}^{2+}$ , which proved the 1 : 1 binding stoichiometry of sensor **Pyr-Rhy** with  $\text{Hg}^{2+}$ . This fluorescent behavior was ascribed to the coordination of sensor **Pyr-Rhy** with  $\text{Hg}^{2+}$ , which decreased the PET process and C=N isomerization. Moreover, there was an excellent linear relationship between the fluorescence intensity

and the concentration of  $\text{Hg}^{2+}$  ( $R^2 = 0.99163$ ) (Fig. 5b). Based on this, the detection limits of sensor **Pyr-Rhy** with  $\text{Hg}^{2+}$  was calculated to be as low as  $2.07 \times 10^{-8}$  M (DL = 3Sb/S).

### 3.3. pH effects

The effect of pH on fluorescence response of sensor **Pyr-Rhy** toward  $\text{Hg}^{2+}$  was determined over a wide range of pH (1.0–14.0). In this test, hydrochloric acid and sodium hydroxide were used to adjust the pH values. As shown in Fig. 6, the fluorescence intensity of sensor **Pyr-Rhy** increased with the increasing of pH value ( $\text{pH} \leq 4.0$ ). And with the increasing of pH ( $\text{pH} = 5\text{--}12$ ), the fluorescence intensity was observed to be held steady. These results proved that this probe has potential application value to test  $\text{Hg}^{2+}$  within a biological scale of pH values.

### 3.4. Competition experiment and reversibility study

High selectivity toward  $\text{Hg}^{2+}$  over the other metal ions is an important parameter, which is helpful to study the performance of sensor **Pyr-Rhy**. Therefore, the competition experiments were carried out in the presence of  $\text{Hg}^{2+}$  (1.0 equiv.) mixed with other metal ions (1.0 equiv.) in aqueous DMSO media (DMSO/ $\text{H}_2\text{O}$ , 1/1, v/v), and the result was shown in Fig. 7. The selectivity of sensor **Pyr-Rhy** toward  $\text{Hg}^{2+}$  ions over other competitive cations was remarkably high, illustrating that sensor **Pyr-Rhy** was capable of fluorescent recognition of  $\text{Hg}^{2+}$  with high selectivity and sensitivity in aqueous DMSO solution (DMSO/ $\text{H}_2\text{O}$ , 1/1, v/v).

Reversibility study was carried out to explore the reuse property of sensor **Pyr-Rhy** toward  $\text{Hg}^{2+}$ . Reversibility is a key prerequisite in designing and developing novel chemosensors for practical applications. The reversibility of the recognition process of sensor **Pyr-Rhy** was performed by adding a strong chelating agent EDA (Fig. 8).<sup>31,32</sup> The addition of excessive EDA to a mixture of sensor **Pyr-Rhy** and  $\text{Hg}^{2+}$  in ethanol solution

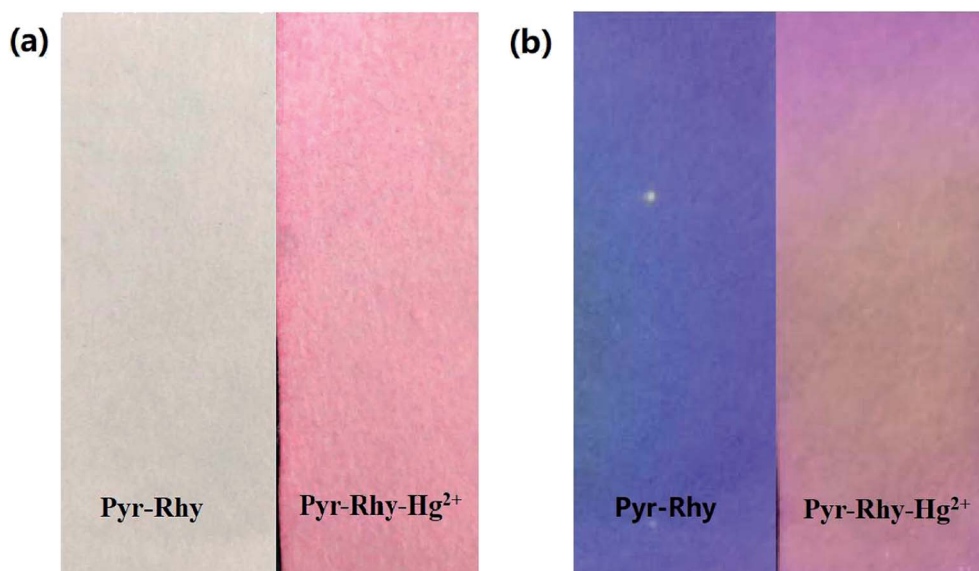


Fig. 9 Photographs showing the color changes of sensor **Pyr-Rhy** before and after addition of  $\text{Hg}^{2+}$  under (a) sunlight and (b) 365 nm UV light.



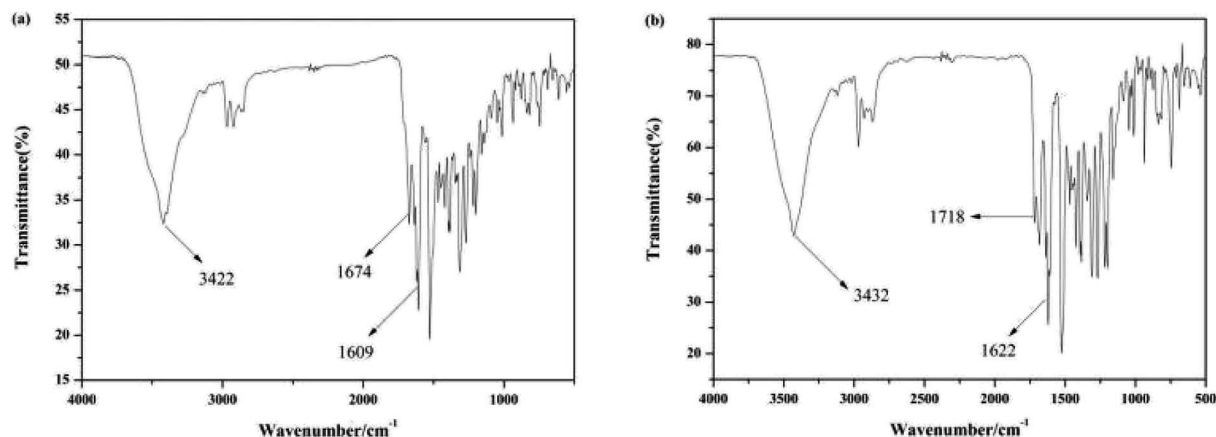


Fig. 10 (a) The FT-IR spectrum of sensor Pyr-Rhy; (b) binding FT-IR spectrum of Pyr-Rhy-Hg<sup>2+</sup>.

resulted in diminution of the fluorescence intensity, due to demetalation of Hg<sup>2+</sup> from the corresponding complex. Meanwhile, the solution color was changed from fluorescent yellow to colorless, which indicated the regeneration of chemosensor Pyr-Rhy. However, when Hg<sup>2+</sup> continued to be added to the mixed solution, a strong fluorescence enhancement was observed and the solution color was changed from colorless to fluorescent yellow, which demonstrated the excellent reversible property of sensor Pyr-Rhy.

### 3.5. Contact mode detection between sensor Pyr-Rhy and Hg<sup>2+</sup>

The recognition of sensor Pyr-Rhy toward Hg<sup>2+</sup> was tested on pretreated filter paper to explore its versatility application as a simple and efficient solid-state probe. The test strips were prepared by immersing the filter paper into a saturated solution of sensor Pyr-Rhy in DMSO for a few seconds. Then, these strips dried in air and subsequently treated with Hg<sup>2+</sup> solution ( $1.0 \times 10^{-3}$  mol L<sup>-1</sup>) in water for solid state experiments. The filter



Fig. 11 <sup>1</sup>H NMR spectra of sensor Pyr-Rhy and complex Pyr-Rhy-Hg<sup>2+</sup> in DMSO-*d*<sub>6</sub>.





Fig. 12 Job's plot for sensor **Pyr-Rhy** and  $\text{Hg}^{2+}$  in DMSO/ $\text{H}_2\text{O}$  (1/1, v/v) solution.

paper soaked with sensor **Pyr-Rhy** ( $1.0 \times 10^{-3} \text{ mol L}^{-1}$ , DMSO as solution) showed white and purple colors under sunlight and 365 nm UV light (Fig. 9), respectively. After soaking with  $\text{Hg}^{2+}$  ( $1.0 \times 10^{-3} \text{ mol L}^{-1}$ , water as solution), the colors were turned to pink and dull red under sunlight and 365 nm UV light, respectively. Therefore, this solid-state method offers a convenient and cost-effective strategy for naked-eye detection of  $\text{Hg}^{2+}$  ion.

### 3.6. Proposed binding mode of sensor **Pyr-Rhy** with $\text{Hg}^{2+}$ ion

The binding mode of sensor **Pyr-Rhy** toward  $\text{Hg}^{2+}$  was investigated through IR spectra (Fig. 10). Free sensor **Pyr-Rhy** showed stretching vibration bands assignable to  $-\text{OH}$  and  $\text{CH}=\text{N}$  at  $3422$  and  $1674 \text{ cm}^{-1}$ , respectively (Fig. 10a). While complexation of sensor **Pyr-Rhy** with  $\text{Hg}^{2+}$  resulted in the obvious shift of  $-\text{OH}$  stretching vibration band from  $3422 \text{ cm}^{-1}$  to  $3432 \text{ cm}^{-1}$  (Fig. 10b). Furthermore, the characteristic stretching vibration band of  $\text{CH}=\text{N}$  and phenolic  $\text{O}-\text{H}$  changed obviously, which indicated that the aldimine nitrogen atom of sensor **Pyr-Rhy** was involved in the chelating with  $\text{Hg}^{2+}$ . This result was further confirmed by the  $^1\text{H}$  NMR spectra recorded in  $\text{DMSO}-d_6$  as

shown in Fig. 11. The H proton signals of phenolic  $\text{OH}$  and aldimine  $\text{CH}=\text{N}$  in free sensor **Pyr-Rhy** were located at  $\delta$  8.74 and 8.50 ppm, respectively. However, upon addition of  $\text{Hg}^{2+}$  (1.0 equiv.), these two signals shifted to lower  $\delta$  values (8.59 ppm for  $\text{OH}$ , and 8.36 ppm for  $\text{CH}=\text{N}$ ). These data strongly supported the previous conclusion that complexation reaction of sensor **Pyr-Rhy** with  $\text{Hg}^{2+}$  occurred at the  $\text{CH}=\text{N}$  position, and thereby leading to the obvious migration of intramolecular electrons and H proton signals of  $\text{CH}=\text{N}$  and  $\text{OH}$ .

In addition, the Job's plot of sensor **Pyr-Rhy** with  $\text{Hg}^{2+}$  in DMSO/ $\text{H}_2\text{O}$  (1/1, v/v) solution was also measured. As depicted in Fig. 12, the maximum emission intensity was measured for a molar fraction of 0.5, which gave a solid evidence for the formation of a 1 : 1 complex of sensor **Pyr-Rhy** with  $\text{Hg}^{2+}$ . Furthermore, the  $R$  value also proved the 1 : 1 stoichiometric ratio for the formation of sensor **Pyr-Rhy**– $\text{Hg}^{2+}$  complex. The 1 : 1 binding stoichiometry was further confirmed by Benesi-Hildebrand method, the plot of  $1/(F - F_0)$  against  $1/[\text{Hg}^{2+}]$  showed an excellent linearity ( $R^2 = 0.99163$ ) (Fig. 5b), which strongly supported the 1 : 1 binding stoichiometry of the sensor **Pyr-Rhy** and  $\text{Hg}^{2+}$ . The proposed binding mechanism of sensor **Pyr-Rhy** with metal ions is shown in Fig. 13.<sup>33–36</sup> Free sensor **Pyr-Rhy** contains two equilibrium conformations owing to the isomerization of  $\text{C}=\text{N}$  bond, which can lead to weak fluorescence emission. After adding specific metal ions, the isomerization of  $\text{C}=\text{N}$  double bond is severely restrained due to the block of photoinduced electron transfer (PET). This process generates a new  $\pi$ -conjugated structure, which can result in the increase of structure rigidity and the enhancement of fluorescence intensity.

## 4. Conclusions

In summary, a novel efficient fluorescent probe **Pyr-Rhy** for naked-eye detection of  $\text{Hg}^{2+}$  had been successfully synthesized, using the commercial available pyrazole and rhodamine 6G as the starting materials. This probe exhibits high anti-interference performance, rapid response, high sensitivity and excellent selectivity toward  $\text{Hg}^{2+}$  over other coexisted metal ions within wide pH range. The filter paper test strips demonstrate that probe **Pyr-Rhy** has high value in the practical applications.

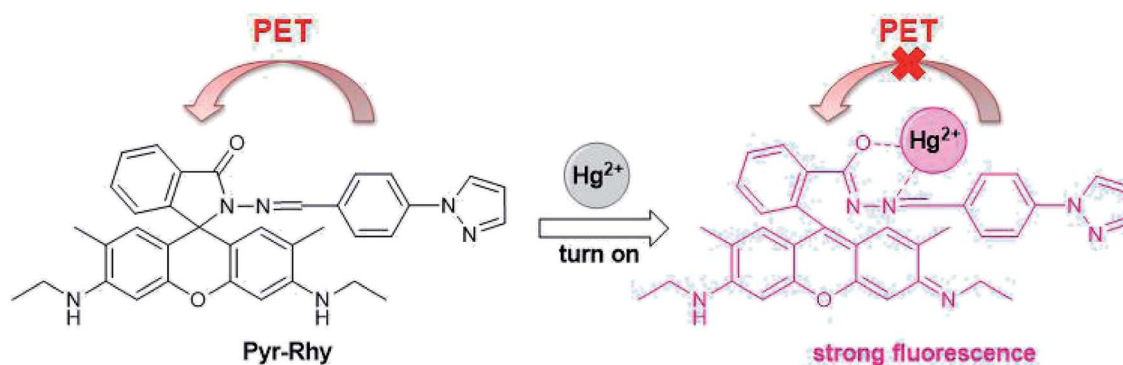


Fig. 13 Proposed sensing mechanism of sensor **Pyr-Rhy** toward  $\text{Hg}^{2+}$ .



Importantly, the probe can be used to trace amounts of hazardous  $\text{Hg}^{2+}$  ions in water with good recoveries and less relative standard deviations, indicating that the developed probe has good accuracy and precision for the analysis of trace  $\text{Hg}^{2+}$  in practical samples.

## Conflicts of interest

The authors declare no competing interests.

## Acknowledgements

This work was funded by the Natural Science Foundation of Shandong Province (No. ZR2018PB007), the Shandong Provincial Natural Science Foundation of China (ZR2017LC005), the Key Research and Development Program of Shandong Province of China (2018 CXGC1107), and the Shandong Provincial Natural Science Foundation of China (ZR2016EMM13).

## References

- 1 N. Schüwer, M.-L. Tercier-Waeber, M. Danial and H.-A. Klok, *Aust. J. Chem.*, 2012, **65**, 1104–1109.
- 2 S. Havarinasab and P. Hultman, *Autoimmun. Rev.*, 2005, **4**, 270–275.
- 3 R. Falter and H. F. Schöler, *J. Chromatogr. A*, 1994, **675**, 253–256.
- 4 P. B. Tchounwou, W. K. Ayensu, N. Ninashvili and D. Sutton, *Environ. Toxicol.*, 2003, **18**, 149–175.
- 5 T. W. Clarkson, L. Magos and G. J. Myers, *N. Engl. J. Med.*, 2003, **349**, 1731–1737.
- 6 T. W. Clarkson and L. Magos, *Crit. Rev. Toxicol.*, 2006, **36**, 609–662.
- 7 M. R. Knecht and M. Sethi, *Anal. Bioanal. Chem.*, 2009, **394**, 33–46.
- 8 G. Hennrich, H. Sonnenschein and U. Resch-Genger, *J. Am. Chem. Soc.*, 1999, **121**, 5073–5074.
- 9 W. Lin, X. Cao, Y. Ding, L. Yuan and L. Long, *Chem. Commun.*, 2010, **46**, 3529–3531.
- 10 Q.-J. Ma, X.-B. Zhang, X.-H. Zhao, Z. Jin, G.-J. Mao, G.-L. Shen and R.-Q. Yu, *Anal. Chim. Acta*, 2010, **663**, 85–90.
- 11 K. Tsukamoto, Y. Shinohara, S. Iwasaki and H. Maeda, *Chem. Commun.*, 2011, **47**, 5073–5075.
- 12 Y. Wang, C. Zhang, X. Chen, B. Yang, L. Yang, C. Jiang and Z. Zhang, *Nanoscale*, 2016, **8**, 5977–5984.
- 13 T. Xuan, X. Yang, S. Lou, J. Huang, Y. Liu, J. Yu, H. Li, K.-L. Wong, C. Wang and J. Wang, *Nanoscale*, 2017, **9**, 15286–15290.
- 14 J. Zhang, L. He, P. Chen, C. Tian, J. Wang, B. Liu, C. Jiang and Z. Zhang, *Nanoscale*, 2017, **9**, 1599–1606.
- 15 L. Wang, W. Qin and W. Liu, *Inorg. Chem. Commun.*, 2010, **13**, 1122–1125.
- 16 H. Miyasaka, N. Matsumoto, H. Ōkawa, N. Re, E. Gallo and C. Floriani, *J. Am. Chem. Soc.*, 1996, **118**, 981–994.
- 17 N. Raman, S. Ravichandran and C. Thangaraja, *J. Chem. Sci.*, 2004, **116**, 215–219.
- 18 M. Guerrero, J. Pons, M. Font-Bardia, T. Calvet and J. Ros, *Aust. J. Chem.*, 2010, **63**, 958–964.
- 19 V. S. Elanchezhian and M. Kandaswamy, *Inorg. Chem. Commun.*, 2010, **13**, 1109–1113.
- 20 A. Ciupa, M. F. Mahon, A. Paul and L. Caggiano, *Org. Biomol. Chem.*, 2012, **10**, 8753–8757.
- 21 B. Willy and T. J. Mueller, *Eur. J. Org. Chem.*, 2008, 4157–4168.
- 22 X.-Y. Wang, C.-G. Niu, L.-J. Guo, L.-Y. Hu, S.-Q. Wu, G.-M. Zeng and F. Li, *J. Fluoresc.*, 2017, **27**, 643–649.
- 23 V. B. Bojinov, A. I. Venkova and N. I. Georgiev, *Sens. Actuators, B*, 2009, **143**, 42–49.
- 24 V. Amendola and M. Meneghetti, *J. Phys. Chem. C*, 2009, **113**, 4277–4285.
- 25 W. Haiss, N. T. Thanh, J. Aveyard and D. G. Fernig, *Anal. Chem.*, 2007, **79**, 4215–4221.
- 26 J. Suurkuusk, B. Lentz, Y. Barenholz, R. Biltonen and T. Thompson, *Biochemistry*, 1976, **15**, 1393–1401.
- 27 B. Ou, M. Hampsch-Woodill and R. L. Prior, *J. Agric. Food Chem.*, 2001, **49**, 4619–4626.
- 28 Y. Chen, C. Zhu, Z. Yang, J. Chen, Y. He, Y. Jiao, W. He, L. Qiu, J. Cen and Z. Guo, *Angew. Chem., Int. Ed.*, 2013, **52**, 1688–1691.
- 29 M. Y. Chae and A. W. Czarnik, *J. Am. Chem. Soc.*, 1992, **114**, 9704–9705.
- 30 L.-J. Fan, Y. Zhang and W. E. Jones, *Macromolecules*, 2005, **38**, 2844–2849.
- 31 S. Zhang, Q. Niu, L. Lan and T. Li, *Sens. Actuators, B*, 2017, **240**, 793–800.
- 32 T. Sun, Q. Niu, Y. Li, T. Li and H. Liu, *Sens. Actuators, B*, 2017, **248**, 24–34.
- 33 L. Lan, Q. Niu, Z. Guo, H. Liu and T. Li, *Sens. Actuators, B*, 2017, **244**, 500–508.
- 34 W. Zhu, L. Yang, M. Fang, Z. Wu, Q. Zhang, F. Yin, Q. Huang and C. Li, *J. Lumin.*, 2015, **158**, 38–43.
- 35 S. Erdemir, S. Malkondu and O. Alici, *Color. Technol.*, 2015, **131**, 32–37.
- 36 H. N. Kim, M. H. Lee, H. J. Kim, J. S. Kim and J. Yoon, *Chem. Soc. Rev.*, 2008, **37**, 1465–1472.

